Evaluating the effects of forest tree species on rill detachment capacity in a semi-arid environment

Evaluating the effects of forest tree species on rill detachment capacity in a semi-arid environment

Misagh Parhizkar [1], Mahmood Shabanpour [1], Isabel Miralles [2], Artemio Cerdà [3], Nobuaki Tanaka [4], Hossein Asadi [5], Manuel Esteban Lucas-Borja [6], Demetrio Antonio Zema [7,]*

[1] Faculty of Agricultural Sciences, University of Guilan, 41635-1314 Rasht, Iran

[2] Department of Agronomy & Center for Intensive Mediterranean Agrosystems and Agri-food Biotechnology (CIAIMBITAL), University of Almeria, E-04120, Almería, Spain.

[3] Soil Erosion and Degradation Research Group (SEDER), University of Valencia, E-46001 Valencia, Spain

[4] Ecohydrology Research Institute, The University of Tokyo Forests, Graduate School of Agricultural and Life Sciences, The University of Tokyo, Seto, Japan

[5] Department of Soil Science, University of Tehran, 11369 Tehran, Iran

[6] Escuela Técnica Superior Ingenieros Agrónomos y Montes, Universidad de Castilla-La Mancha, Campus Universitario, E-02071 Albacete, Spain

[7] Department AGRARIA, Mediterranean University of Reggio Calabria, Loc. Feo di Vito, I-89122 Reggio Calabria, Italy

* Correspondence: dzema@unic.it

Abstract

The beneficial effects of plant roots in decreasing soil detachment in forest ecosystems exposed to rill erosion are well known. However, these effects vary largely between different plant species. There has been lots of research into the relationship between root-soil systems and rill erodibility with a particular focus on grass species. Conversely, fewer studies are available for tree species, especially in forests of semi-arid or arid environments. Greater knowledge is therefore needed to identify the most effective tree species against rill erosion in these ecosystems, where water availability is the limiting factor for vegetation growth and afforestation is often the only solution to control erosion. To fill this gap, this study evaluates the rill detachment capacity of soils with four tree species (*Parrotia persica, Carpinus betulus, Quercus castaneifolia,* and *Pinus taeda*) in a semi-arid forest ecosystem in Northern Iran. These species are typical of these forests, but they also grow in other environmental contexts. The rill detachment was simulated in a laboratory flume at five slope gradients (1% to 5%) and five flow rates (0.22 to 0.69 L m^{-1} s^{-1}) on soil samples with each of the tree species. The specific goal of the study was to evaluate which tree species with its specific root characteristics is most effective at reducing the rill detachment capacity. Moreover, simple prediction models are proposed to evaluate if it is possible to estimate the rill detachment capacity and rill erodibility (K_r) from the unit stream power for the investigated tree species. The soils with *Parrotia persica* and *Carpinus betulus* showed the lowest and the highest rill detachment capacity, respectively. The higher root system biomass of *Parrotia persica* could have played a binding effect on the soil, thus improving its aggregate stability thanks to the action of plant's root system. Based on these results, *Parrotia persica* is able to provide a higher soil protection capacity against erosion compared to the other tree species. A logarithmic function was accurate in predicting the rill detachment capacity from the unit stream power at water flow rates over 0.0025 m s^{-1}. By a regression between the rill detachment capacity and the shear stress of the soil, rill erodibility and critical shear stress of soils were estimated for the four tree species; the rill erodibility and critical shear stress are important input parameters for physically-based erosion models. Overall, the results of this study can support land planners in the choice of tree species most indicated for soil conservation as well as in the extensive application of erosion prediction models.

Keywords: forest; *Parrotia persica*; rill erodibility; unit stream power; root density; shallow flow; soil erosion.

1. Introduction

Soil erosion is a complex environmental process, consisting of detachment from place, transport, and deposition of soil particles, often at a long distance (Ellison, 1947; Prosdocimi et al., 2016). Soil detachment is due to rainsplash and overland flow (Govers et al., 1990), which are the main soil detachment mechanisms in inter-rill and rill erosion, respectively (Zhang et al., 2003). Regarding rill erosion, its maximum value at zero sediment concentration is called “soil detachment capacity” (Foster, 1982). This is the most important parameter drivingsoil resistance to water erosion, particularly on steep slopes (Wang et al., 2018b; Owoputi and Stolte, 1995). Regarding concentrated flow erosion, this process is driven by "soil detachment capacity by rill flow" or, more simply, “rill detachment capacity” (hereinafter indicated by "D_c"). Therefore, it is essential to quantify which factors influence soil detachment capacity, in order to control and limit erosion by appropriate soil management practices. In general, these practices are based on increasing vegetal cover and/or modifying soil properties (Cerdà et al., 2016).

For technical, economic or legal reasons, it is not always easy to modify soil properties. The use of vegetation with tree or herbaceous species is a more viable solution to control surface erosion on hillslopes, reducing the soil erodibility. Revegetation for erosion control is based on the effects of the above-ground biomass; the latter, however, can temporally disappear, because of fire, overgrazing or concentrated erosion, particularly in arid and semi-arid areas (De Baets et al., 2007). In these environments, the importance of below-ground biomass that can effectively control soil erosion rates is often neglected. The beneficial effects of an extensive vegetal cover against soil erosion are many: the reduction of surface runoff volume and velocity (Fiener and Auerswald, 2003; Koskiaho, 2003; Li et al., 2013), the increase in water infiltration (De Baets et al., 2008; Li et al., 1992; 1995), and bonding of soil particles at the soil surface (De Baets et al., 2006; 2007). Most of these effects are due to the plant root system and are essential, particularly on steep slopes and with loose soils, since plant roots reduce the sediment detachment by increasing the shear strength of the root-soil matrix (Abdi et al., 2010; Herbrich et al., 2018; Wang et al., 2018a). However, these effects vary largely depending on the different characteristics of the vegetation (tree, shrub or, grass layer; plant species; environmental conditions) (Jiao et al., 2008), and particularly on the size, distribution and density of the plant roots (De Baets et al., 2007b; Gyssels et al., 2005). Based on the characteristics of the root system, the most suitable plant species for erosion control can be properly selected to achieve a reduction in soil erosion (Pollen, 2007). Among the root system characteristics, the root system biomass (that is, the dry mass of roots in the soil) has been used by many authors as a key driver in reducing soil detachment (Wang et al., 2014b; Li et al., 2015; Wang et al., 2018a; 2018b; Parhizkar et al., 2020b). For example, Wang et al. (2014a; 2014b) found that root density is the most influential factor on soil detachment capacity because of its physical and chemical binding effects (De Baets et al., 2006; Zhang et al., 2013). De Baets et al. (2007) showed that root density is correlated to soil detachment rate by a negative exponential equation. Unfortunately, information on the effects of plant roots on topsoil resistance to rill erosion is not sufficient (De Baets et al., 2007). A large variety of tree species exist, and each species has its own specific root system characteristics. Previous studies have demonstrated that different tree species exert different influences on the physico-chemical properties of soils (e.g., Gyssels et al., 2005; Meek et al., 1992; Keller and Håkansson, 2010; Gyssels and Poesen, 2003; Shabanpour et al., 2020), but particularly on soil detachment capacity (Wang et al, 2014a; Zhang et al, 2013; Mamo and Bubenzer, 2001a; 2001b).

The studies that have evaluated the effects of plant root systems on soil erodibility and rill detachment capacity have been carried out in specific environments (e.g., Loess Plateau in China, Wang et al., 2014b; 2018a) and at the landscape scale (e.g., Li et al., 2015; Geng et al., 2021, again in Loess Plateau) or have mainly focused on shrub and grass species (e.g., De Baets et al., 2006; Zhang et al., 2013; Wang et al., 2021). In general, all these studies have highlighted that the detachment rate of rooted soils is reduced compared to other soils, with consequent increased soil stability (e.g., Mamo and Bubenzer 2001a; 2001b), since erodibility is greatly reduced (even by more than 80-90%) compared to bare or deforested soils (Wang et al., 2014a; Parhizkar et al., 2020b).

Some authors have also demonstrated that the effects of plant roots on soil erosion vary depending on the plant species (Wang et al., 2018b) and the hydraulic parameters of the water flow and soil properties (Gyssels et al., 2005). Despite this large body of literature, less attention has been paid to tree species and, especially, to forest ecosystems, which, in some environmental contexts (steep slopes and arid or semi-arid climate) may be particularly prone to rill erosion. In fact, rill erosion is the most important erosive process on hillslopes with a high gradient (Wang et al., 2014b; Owoputi et al., 1995), and semi-arid and arid climates - such as the Mediterranean Basin - are characterized by heavy rainstorms, resulting in highly concentrated runoff rates with high erosion power (Fortugno et al., 2017). Forest cover with trees that have a well-developed root system is highly effective at reducing soil erosion (Gyssels et al., 2005; Parhizkar et al., 2020b). Moreover, afforestation with tree species is often the only solution for reducing soil erosion in arid or semi-arid ecosystems, where water availability is the limiting factor for vegetation growth (Querejeta et al., 2001). Therefore, more research is needed to understand how a given forest tree species with a root system having specific biomass characteristics drives the soil detachment process. In other words, there is a need to evaluate the soil detachment capacity under an individual plant species and different soil and hydraulic conditions. Such evaluations are useful to select the most effective tree species for afforestation in steep hillslopes with high erosion rates (Norris et al., 2008; Perez et al., 2017).

To fill these gaps, this study quantifies the rill detachment capacity in soils sampled under four species of adult trees (*Parrotia persica, Quercus castaneifolia, Pinus taeda* and *Carpinus betulum*) in Saravan Forest Park (Northern Iran), using an experimental flume. Moreover, simple models are proposed for the specific environmental conditions and tree species, to predict the soil detachment capacity and rill erodibility. This investigation adds the effect of the plant components to the results of a previous study by Parhizkar et al. (2020a), carried out at the landscape scale under the same experimental conditions. These authors showed that: (i) the soil detachment capacity of concentrated flow is lower in forests and woodlands compared to grasslands and croplands; (ii) the unit stream power of water flow is a very accurate predictor of soil detachment capacity. Following this approach, our research questions were the following: (i) Which tree species with its specific root system is more able to reduce the rill detachment capacity?; (ii) Are the prediction models proposed by Parhizkar et al. (2020a) also valid at a smaller scale for the analyzed tree species?

2. Materials and methods

2.1. Study area

The province of Guilan (Northern Iran) lies between the southern coast of the Caspian Sea and the northern part of the Alborz Mountains. The landscape of this province consists of a green belt of old-growth Hyrcanian forests with high diversity of tree species and plant communities (Amoopour et al., 2016). According to Parhizkar et al. (2020a), special attention must be paid to the forests of this province, where existing problems of erosion may increase if soil conservation issues are neglected.

The experimental site is located in Saravan Forest Park, which is one of the oldest forests in Guilan province (outlet coordinates 37°08'04" N, 49°39'44" E). The park drains the Saravan watershed (coordinates 37°08'04" N, 49°39'44" E), which covers an area of 14.87 km^2 at an elevation from 50 to 250 m (Figure 1).

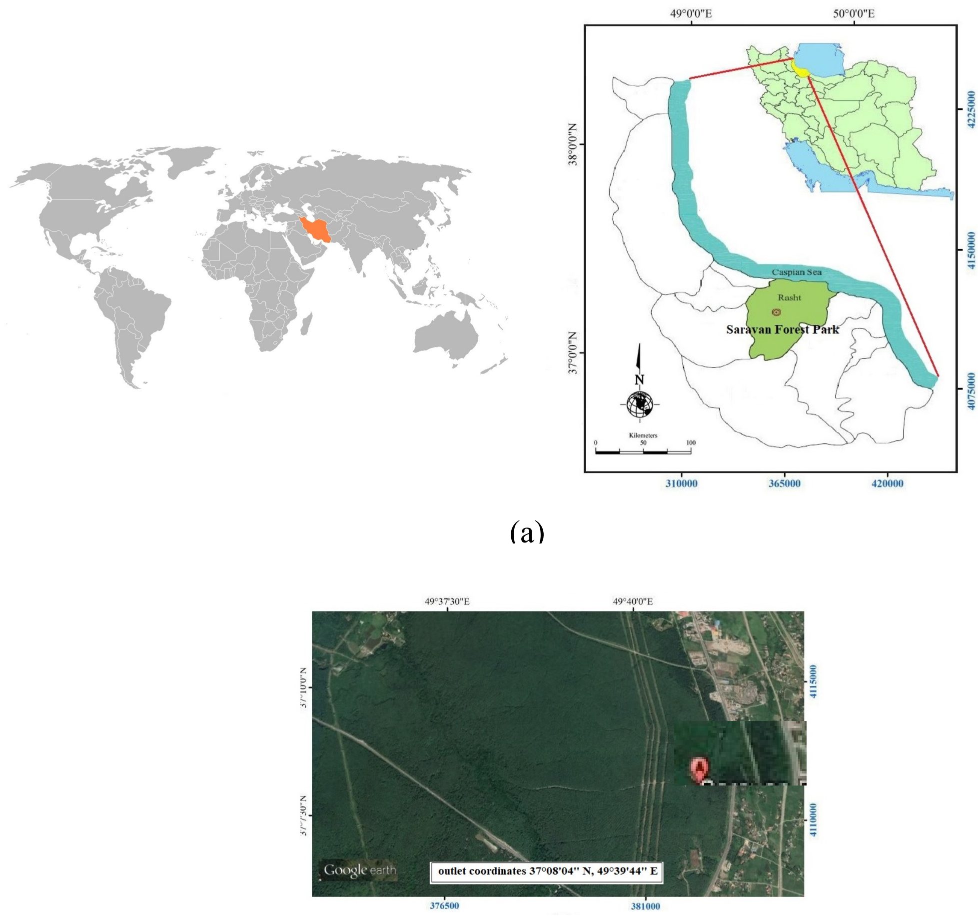

Figure 1 - Geographical location (a) (source: Google Earth, 2020) and aerial map (b) in the study area (Saravan Forest Park, Northern Iran).

This area has a Mediterranean climate, *Csa* type, according to the Köppen–Geiger classification (Kottek et al., 2006). The mean annual precipitation and temperature are 1360 mm and 16.3 °C, respectively (IRIMO, 2016); precipitation is mainly concentrated in the coldest months and scarce in the dry period (Figure 1(SD)).

The Saravan watershed features an abundant biodiversity of forest plants, including 80 tree and shrub species (Sagheb-Talebi, et al., 2005; Hosseini, 2003, Kartoolinejad, et al., 2007). The dominant tree species are *Carpinus betulus* L. (C. betulus), *Quercus castaneifolia* C.A.Mey. (Q. castaneifolia), *Pinus taeda* L. (P. taeda), and *Parrotia persica* C.A.Mey. (P. persica) (Picchio et al., 2020; Mirabolfathy et al., 2018; Payam and Pourrajabali, 2020; Karimi et al., 2018). These species are typical of Northern Iran but grow throughout the Southern Caspian area (*P. persica* and *Q. castaneifolia* are also well diffused in Turkey and Azerbaijan), South-eastern United States (*P. taeda*), and Western Asia and Central, Eeastern, and Southern Europe (*C. betulus*). Other shrub and herbaceous species in the area are *Artemisia annua* L., *Cynodon dactylon* (L.) *Pers.*, *Hedera helix* L., *Hedera pastuchovii Woron. Ex* Grossh., *Hypericum androsaemum* L., *Hypericum perforatum* L., *Juncus bufonius* L., *Juncus glaucus* Ehrh., *Mentha pulegium* L., *Morus alba* L., *Primula heterochoroma* Starf., *Prunus domestica* L., *Scutelaria albida* L., and *Solanum dulcamara* L.

Regarding the tree species, *P. persica* is a deciduous tree from Hamamelidaceae family, specifically native tonorthern Iran (Sefidi et al., 2011; Karimi et al., 2018). This is a highly ornamental tree or large shrub that can grow at an altitude of 20-25 m and tolerates drought, heat, wind and cold (Gilman, 2014). *C. betulus* is a semi-shade tolerant species (Marvie-Mohadjer, 2019), while *P. taeda* is an exotic and fast growing coniferous species (Picchio et al., 2020), which is used for commercial plantations. *Q. castaneifolia* is one of the most important native oak species of Iran (Payam and Pourrajabali, 2020). Table 1 showsthe main physiological characteristics of these tree species surveyed in the study area.

Table 1 – Main physiological characteristics (mean ± std. dev.) of the forest tree species surveyed in the study area (Saravan Forest Park, Northern Iran).

Tree species	**Height (m)**	**Diameter[(*)] (m)**	**Cover (%)**
Parrotia persica	19 ± 0.6	0.57 ± 0.03	40
Pinus taeda	16 ± 0.3	0.26 ± 0.03	30
Carpinus betulus	22 ± 0.7	0.60 ± 0.04	15
Quercus castaneifolia	23 ± 0.7	0.61 ± 0.04	15

Note: (*) measured in this study at breast height.

Four mixed forests, with *C. betulus, Q. castaneifolia*, *P. taeda* and *P. persica* as prevalent species in areas with the same slope gradient were selected for this study (Abedi and Pourbabaei, 2011; Amoopour et al., 2016). On average, the *C. betulus* and Q. castaneifolia species each cover 15% of the area, while P. persica and *P. taeda* are the dominant species on 40% and 30% of the total area, respectively (Table 1). All the species are less than 15-20 years old. *P. persica* shows a fibrous root system growing horizontally in the soil (Abdi et al., 2014). By contrast, *Q. castaneifolia*, *P. taeda*, and *C. betulus* have deep taproot systems, and their roots grow vertically along the soil profile (Hacke et al., 2000; Rewald et al., 2016; Abdi and Deljouei, 2019). *C. betulus* has the largest and deepest root system with the coarsest root diameter (Kooch et al., 2016; Bonyad, 2006). About ten years ago, some of the hillslopes in Saravan Park were deforested to install high-voltage electricity pylons, with high density tree and plant cover being totally removed (Parhizkar et al., 2020b). This deforestation induced intense rill erosion (Figure 2), meaning management action is absolutely necessary to avoid further biodiversity losses.

(a) *(b)*

Figure 2 - Views of rill erosion on hillslopes with previous cover of *Quercus castaneifolia* after deforestation (Saravan Forest Park, Northern Iran) - (a, aerial view using a drone, and b, front view).

2.2. Soil sampling procedure

To measure the rill detachment capacity of the soil (D_c), between October and November 2019 undisturbed samples were collected in each of the areas with a dominant species among *P. persica*, *P. taeda*, *C. betulus*, and *Q. castaneifolia*. Five samples were collected around five trees for each species. For each tree, two quadrats (1 x 1 m and 2 x 2 m) were overlaid on the ground. Two samples were collected in the vertices of the diagonal of the first quadrat, and two others were collected in the vertices of the opposite diagonal of the second quadrat. The fifth sample was collected immediately beside the trunk. This design allowed sampling in different positions (two opposite diagonals) and three distances from the tree (0, 0.7 and 1.4 m).

The sampling procedure, adapted to this study from the works of Zhang et al. (2003; 2008), is described in more detail in the paper by Parhizkar et al. (2020a). To summarise, the samples were extracted from the soil using a steel ring (diameter of 0.1 m and height of 0.05 m), after removing rocks, weeds, and litter from the soil surface. Then the soil cores in the ring were transported to the laboratory, with the maximum care, to avoid soil disturbance.

2.3. Soil analyses

An additional set of 100 soil samples (25 samples × 4 tree species) was randomly collected in the same locations, to measure the root system biomass (RSB, by the washing method over a 1-mm sieve and subsequent oven drying at 65 °C), soil content of organic matter (OM, by the potassium dichromate colorimetric method), aggregate stability in water of soil (AS, De Leenheer and De Boodt, 1959), and bulk density (BD) (both using the wet-sieving and oven-drying methods).

2.4. Measurement of rill detachment capacity

A laboratory-scale flume with a rectangular cross section (length of 0.5 m and width of 0.2 m) was used to generate rill flow to evaluate the rill detachment capacity (D_c, [kg s^{-1} m^{-2}]) of soil samples for each tree species at different values of flow rate and soil slope. Each "experiment" was a combination of flow rate, slope gradient, and species simulated in the flume, of which a complete description is reported in Asadi et al. (2011), Raei et al. (2015), and Parhizkar et al. (2020a).

To summarise, each soil core was collected using a steel ring (Section 2.2) and inserted in a hole of the flume bed, close to the downstream outlet, with the sample's upper surface adjusted to the same level as that of the flume bed surface. Then the flow rate and flume profile slope were adjusted to the desired values. Using clean water fed upstream of the flume, D_c and the hydraulic parameters of the water flow (Section 2.6) were measured over a 5–300 second period. The experimental test ended when the depth of the eroded soil in the steel ring reached 0.015 m. After each test, the sample of wet soil was oven dried at 105 °C for 24 h to determine its dry weight.

After the start of each experiment in the flume, we expected that the flow would become steady. Then, using a level probe (accuracy of 1 mm), the water depth (h, [m]) was measured at three points (0.01 m from the right and left sides and in the middle for each of two cross sections, located at 0.4 m and 1 m from the flume outlet). Then the mean flow depth was calculated as the average value of these six measurements.

D_c was calculated as the average value of four replicates using equation (1):

$$D_c = \frac{\Delta M}{A \cdot \Delta t} \tag{1}$$

where:

- ΔM [kg] = dry weight of detached soil
- Δt [s] = experiment duration [s]
- A [m^2] = area of soil sample.

2.5. Experimental design

For each soil sample of the four plant species (*C. betulus*, *Q. castaneifolia*, *P. taeda*, and *P. persica*), five water flow rates per unit width (*q*, 0.26, 0.35, 0.45, 0.56, and 0.67 L m^{-1} s^{-1}) and five slope gradients (*S*, 1%, 2%, 3%, 4%, and 5%) were simulated in the flume, and each experiment consisted of four replicates. Overall, 400 soil samples (4 plant species × 5 water flow rates × 5 slope gradients × 4 replications) were subjected to the experiments.

2.6. Determination of the hydraulic parameters

The values of *q* were measured five times per experiment (collecting the water into a graduated plastic cylinder), while the water velocity (*v,* [m s^{-1}]) was estimated using the fluorescent dye technique in ten replicated measurements. Water viscosity was computed from the temperature. The mean velocity (*V,* [m s^{-1}]) was calculated reducing *v* by 0.6, 0.7, or 0.8, when the flow was laminar, transitional or turbulent, respectively (Abrahams et al., 1985).

In accordance with several authors (Nearing et al., 1997), *R*, *Re*, τ (Foster, 1982), Ω (Bagnold, 1966), and ω (Yang et al., 1972) were calculated using the following equations:

$$R = \frac{h \cdot p}{2p + h} \tag{2}$$

$$\tau = \rho g R S \tag{3}$$

$$\Omega = \rho g S q \tag{4}$$

and

$$\omega = SV \quad (5)$$

where:

- g = gravity acceleration [m s^{-2}]
- p = flume width [m]
- R = hydraulic radius [m]
- Re = Reynolds number [–]
- α = kinetic energy correction (in this case assumed as one)
- ρ = water density [kg m^{-3}]
- ω = unit stream power [m s^{-1}]
- Ω = stream power [kg s^{-3}].

The values of the hydraulic parameters calculated for each flow rate and profile slope in the experimental flume are reported in Table 2(SD) of the Supplementary Data.

2.7. Modelling of rill detachment capacity and rill erodibility

The measured values of D_c (considered as the dependent variable) were regressed on ω (independent variable) using linear and non-linear equations (the latter with power or logarithmic functions) for each tree species, to identify the most accurate predictive model. The accuracy of these equations was checked using a set of statistics (mean, standard deviation, minimum and maximum values), and summary and difference indexes: the coefficient of determination (R^2), coefficient of efficiency (E), root mean square error (RMSE), and coefficient of residual mass (CRM). The equations to calculate these indexes with the acceptance limits are reported in Table 2 (Zema et al., 2012; Krause et al., 2005; Moriasi et al., 2007; Van Liew and Garbrecht, 2003).

Table 2 - Indexes and related equations, and range of variability to evaluate the prediction capacity of the models.

Index	Equation	Range of variability	Acceptance limit and notes
Coefficient of determination (R^2)	$r^2 = \left[\frac{\sum_{i=1}^{n} (O_i - \overline{O})(P_i - \overline{P})}{\sqrt{\sum_{i=1}^{n} (O_i - \overline{O})^2} \sqrt{\sum_{i=1}^{n} (P_i - \overline{P})^2}} \right]^2$	0 to 1	> 0.5 (Santhi et al., 2001; Van Liew et al., 2003; Vieira et al., 2018)
Coefficient of efficiency (E, Nash and Sutcliffe, 1970)	$E = 1 - \frac{\sum_{i=1}^{n} (O_i - P_i)^2}{\sum_{i=1}^{n} (O_i - \overline{O})^2}$	-∞ to 1	"Good" model accuracy if E ≥ 0.75, "satisfactory" if 0.36 ≤ E < 0.75 and "unsatisfactory" if E < 0.36 (Van Liew and Garbrecht, 2003)
Root mean square error (RMSE)	$\mathrm{RMSE} = \sqrt{\frac{\sum_{i=1}^{n} (P_i - O_i)^2}{n}}$	0 to ∞	< 0.5 of observed standard deviation (Singh et al., 2004)
Coefficient of residual mass (CRM or PBIAS, Loague and Green, 1991)	$\mathrm{CRM} = \frac{\sum_{i=1}^{n} O_i - \sum_{i=1}^{n} P_i}{\sum_{i=1}^{n} O_i}$	-∞ to ∞	< 0.25 (Moriasi et al., 2007) - CRM < 0 indicates model underestimation - CRM > 0 indicates model overestimation (Gupta et al., 1999)

Notes: n = number of observations; O_i, P_i = observed and predicted values at the time step i; $\overline{O}$ = mean of observed values.

Finally, the rill erodibility (K_r , [s m^{-1}]) was estimated as the slope and intercept of equation (6) (Nearing et al., 1989):

$$D_C = K_r(\tau - \tau_c) \tag{6}$$

where:

- τ = hydraulic shear stress [Pa]
- τ_c = critical shear stress [Pa]

2.8. Statistical analysis

The statistical significance ($p < 0.05$) of the differences in the soil properties among the tree species was evaluated using the *t*-test. The samples were assumed to be independent, and their distribution was checked by QQ-plots.

Then, the analysis of covariance (ANCOVA) was applied to D_c (dependent variable), using the tree species (categorical variable), and the slope and flow rate (numerical variables) as factors. The pairwise comparison by Tukey's test (at $p < 0.05$) was also used to evaluate the statistical significance of the differences in D_c among the tree species. To satisfy the assumptions of the statistical tests (equality of variance and normal distribution of samples), the data were subjected to a normality test or were square root-transformed whenever necessary.

Finally, Pearson's matrix was calculated to find correlations among the soil properties. The principal component analysis (PCA) was also applied to the soil properties to select a few derivative parameters and to cluster soil samples in groups related to each tree species.

All statistical analyses were conducted by XLSTAT 9.0 software (Addinsoft, Paris, France).

3. Results

3.1. Variability of soil properties and rill detachment capacity among the tree species

The texture of the soil samples was silty clay loam (according to the USDA classification, 33% clay, 46% silt, and 19% sand), without significant variations among the tree species. The differences in texture and bulk density (on average 1359 kg m^{-3}) of the soil samples were not significant (Table 3). Conversely, the other soil properties were in general significantly different among the tree species. More specifically, the aggregate stability was higher (0.72 ± 0.05) in *P. persica* and lower (0.48 ± 0.06) in *C. betulus* The latter species showed the lowest root system biomass (0.51 ± 0.03 kg m^{-3}), while the maximum value

(0.87 ± 0.02 kg m^{-3}) was recorded in *C. betulus* Organic matter was 1.63 ± 0.01% in *C. betulus*, 1.73 ± 0.01% in Q. castaneifolia, 1.96 ± 0.01% in *P. persica*, and 1.84 ± 0.02 in *P. taeda* The differences in OM content among the species were significant, except for *C. betulus* and *Q. castaneifolia* (Table 1).

Table 3 - Main properties (mean ± standard deviation) of forest soil sampled under four tree species in Saravan Forest Park (Northern Iran).

Soil property		**Tree species**			
		C. betulus	*Q. castaneifolia*	*P. persica*	*P. taeda*
Texture (%)	*ClC*	33.8 ± 0.33 a	33.7 ± 0.46 a	33.5 ± 0.24 a	33.5 ± 0.23 a
	SiC	46.9 ± 0.61 a	46.8 ± 0.60 a	46.7 ± 0.35 a	46.9 ± 0.35 a
	SaC	19.3 ± 0.47 a	19.5 ± 0.25 a	19.8 ± 0.25 a	19.6 ± 0.23 a
BD (kg m^{-3})		1384 ± 12.29 a	1366 ± 10.50 a	1331 ± 13.99 a	1355 ± 11.73 a
RSB (kg m^{-3})		0.51 ± 0.03 a	0.62 ± 0.02 b	0.87 ± 0.02 c	0.70 ± 0.07 b
AS (-)		0.48 ± 0.06 a	0.55 ± 0.04 a	0.72 ± 0.05 b	0.61 ± 0.06 c
OM (%)		1.63 ± 0.01 a	1.73 ± 0.01 a	1.96 ± 0.01 b	1.84 ± 0.02 c

Notes: OM = organic matter content; BD = bulk density; RSB = root system biomass; AS = aggregate stability; SaC = sand content; SiC = silt content; ClC = clay content; the letters indicate significant differences among tree species at $p < 0.05$ of the *t*-test ($n = 25$ for each species).

D_c was significantly influenced by the tree species ($p < 0.05$). The mean value was the highest for *C. betulus* (0.00336 kg m^{-2} s^{-1}) and the lowest for *P. persica* (0.00226 kg m^{-2} s^{-1}). Therefore, the ratio between the maximum and minimum D_c was on average 1.49. Q. castaneifolia and *P. taeda* had intermediate D_c (0.0031 and 0.0026 kg m^{-2} s^{-1}, respectively) between the extreme values. The variability of D_c is noticeable among the tree species, as shown by coefficients of variation (ratio of standard deviation by mean) between 78.4% (*C. betulus*) and 92.9% (*P. persica*) (Figure 3).

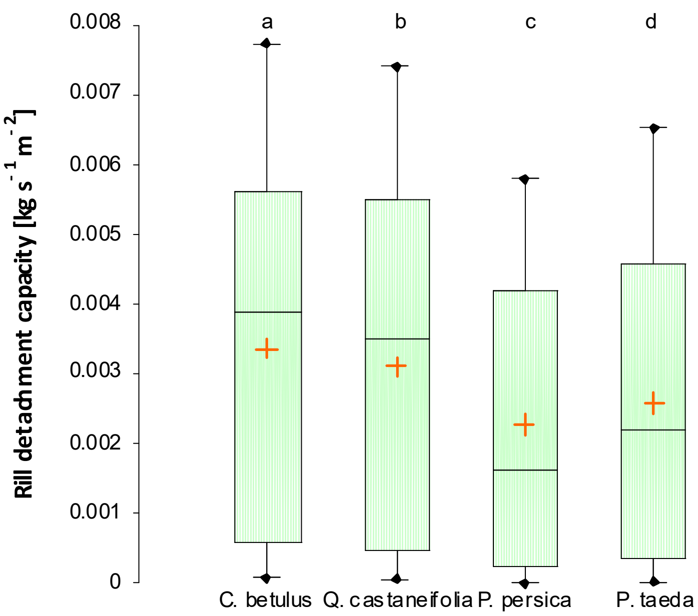

Different letters indicate significant differences after ANOVA at p < 0.05.

Figure 3 - Box-whisker plot of rill detachment capacity in forest soils sampled under four tree species in Saravan Forest Park (Northern Iran) (*n* = 25 for each species).

Pearson's matrix shows that the correlations of D_c with the other soil properties were generally low (coefficient of correlation R < 0.27) and significant only with the root system biomass (R = –0.257) and aggregate stability (R = –0.261). Conversely, the correlations between the other pairs of soil properties were high and significant. For instance, the organic matter content was correlated with the root system biomass (R = 0.942), aggregate stability (R = 0.837), and bulk density (R = –0.843). Moreover, the correlations among the latter soil properties were also high (R = –0.789 between the bulk density and the root system biomass, –0.686 between the bulk density and the aggregate stability, and 0.840 between the root system biomass and the aggregate stability). As regards the soil texture, only the silt content was significantly correlated with sand (R = –0.507) and clay (R = –0.470), although *R* was not high (Table 4).

Table 4 - Pearson's correlation matrix among the properties of forest soils sampled under four tree species (*n* = 25 for each species) in Saravan Forest Park (Northern Iran).

Soil property	D_c	OM	BD	RSB	AS	SaC	SiC	ClC
D_c		−0.159	−0.045	**−0.257**	**−0.261**	−0.057	0.097	0.083

OM			**−0.843**	**0.942**	**0.837**	0.230	**−0.289**	−0.141
BD				**−0.789**	**−0.686**	−0.237	0.240	0.174
RSB					**0.840**	0.220	−0.243	−0.143
AS						0.135	−0.222	−0.079
SaC							**−0.507**	0.059
SiC								**−0.470**
ClC								

Notes: D_c = rill detachment capacity; OM = organic matter content; BD = bulk density; RSB = root system biomass; AS = aggregate stability; SaC = sand content; SiC = silt content; ClC = clay content; values in bold are different from 0 at p level < 0.01.

PCA provided three principal components (PCs), which explained 48.7% (PC_1), 24.7% (PC_2), and 13.0% (PC_3) of the total variance of the properties of the soils collected under the four tree species. The first two PCs explained 73.3% of this variance. The properties related to the soil texture had significant loadings on PC_2 (very high for clay, over 0.90). The other soil properties significantly influenced the first PC with high loadings (over 0.75), while D_c heavily weighed on PC_3 (loading of 0.92) (Table 5). In other words, these loadings confirm the results of Pearson's correlations (high r coefficients and therefore strong associations among organic matter, bulk density, root system biomass, and aggregate stability), but no direct association was found between D_c and the other soil properties (Table 5 and Figure 4a).

Table 5 **-** Loadings of the original variables (properties of forest soils collected under four tree species) on the first two principal components (PC_1 and PC_2) (n = 25 for each species in Saravan Forest Park, Northern Iran).

Soil properties	**Principal components**		
	PC_1	PC_2	PC_3
D_c	0.053	0.000	**0.921**
OM	**0.928**	0.010	0.003
BD	**0.754**	0.002	0.091
RSB	**0.901**	0.011	0.004
AS	**0.782**	0.008	0.013

SaC	0.342	**0.332**	0.005
SiC	0.050	**0.945**	0.000
ClC	0.083	**0.665**	0.005

Notes: D_c = rill detachment capacity; OM = organic matter content; BD = bulk density; RSB = root system biomass; AS = aggregate stability; SaC = sand content; SiC = silt content; ClC = clay content; values in bold correspond for each variable to the factor for which the loading is the largest.

The plot of the sample scores on the first three PCs shows clear differences in soil properties among the studied tree species. Four well-differentiated groups, one for each tree species, are evidenced, with only a limited overlapping of groups for the *P. taeda* and Q. castaneifolia species (Figure 4b).

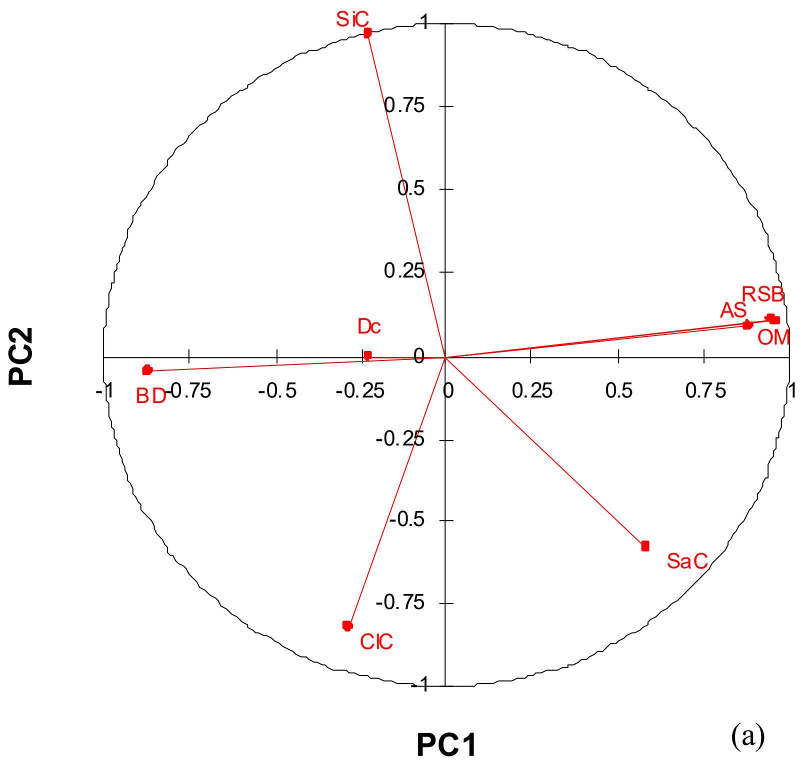

(a)

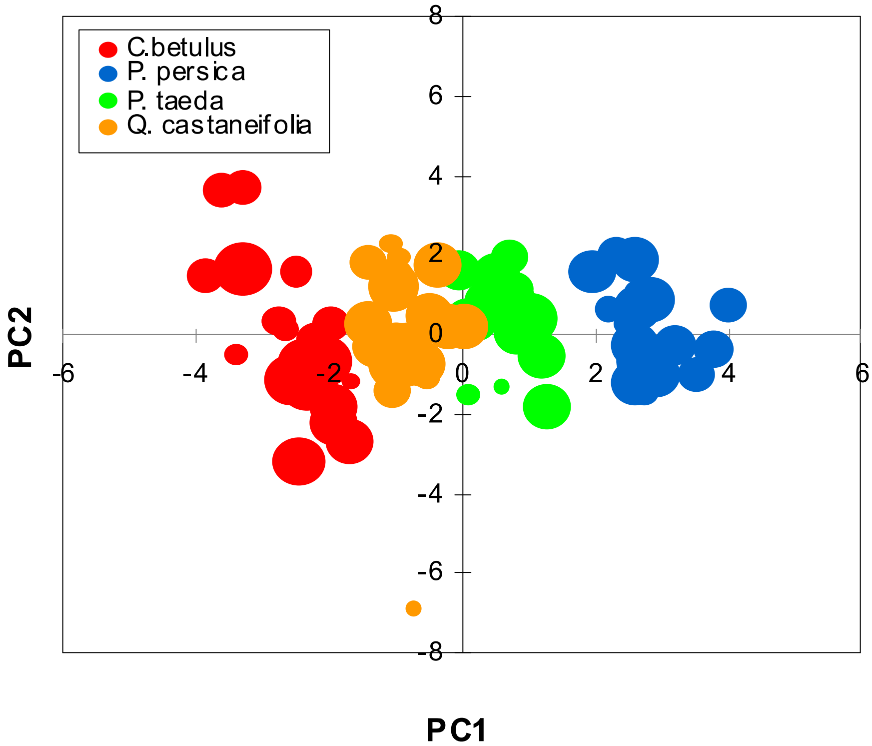

(b)

Legend: D_c = rill detachment capacity; OM = organic matter content; BD = bulk density; RWD = root system biomass; AS = aggregate stability; SaC = sand content; SiC = silt content; ClC = clay content: PC = principal component.

Figure 4 - Loadings of soil parameters (a), and scores of forest soil samples (b) on the first two principal components (PC) for four tree species in Saravan Forest Park (Northern Iran). (The circle size is proportional to the values of the third PC.)

3.2. Relationships among rill detachment capacity and unit stream power and estimation of rill erodibility

Figure 5 shows that at low values of the unit stream power ω (< 0.005–0.006 m s^{-1}) the differences in D_c were small; moreover, these differences increased with ω.

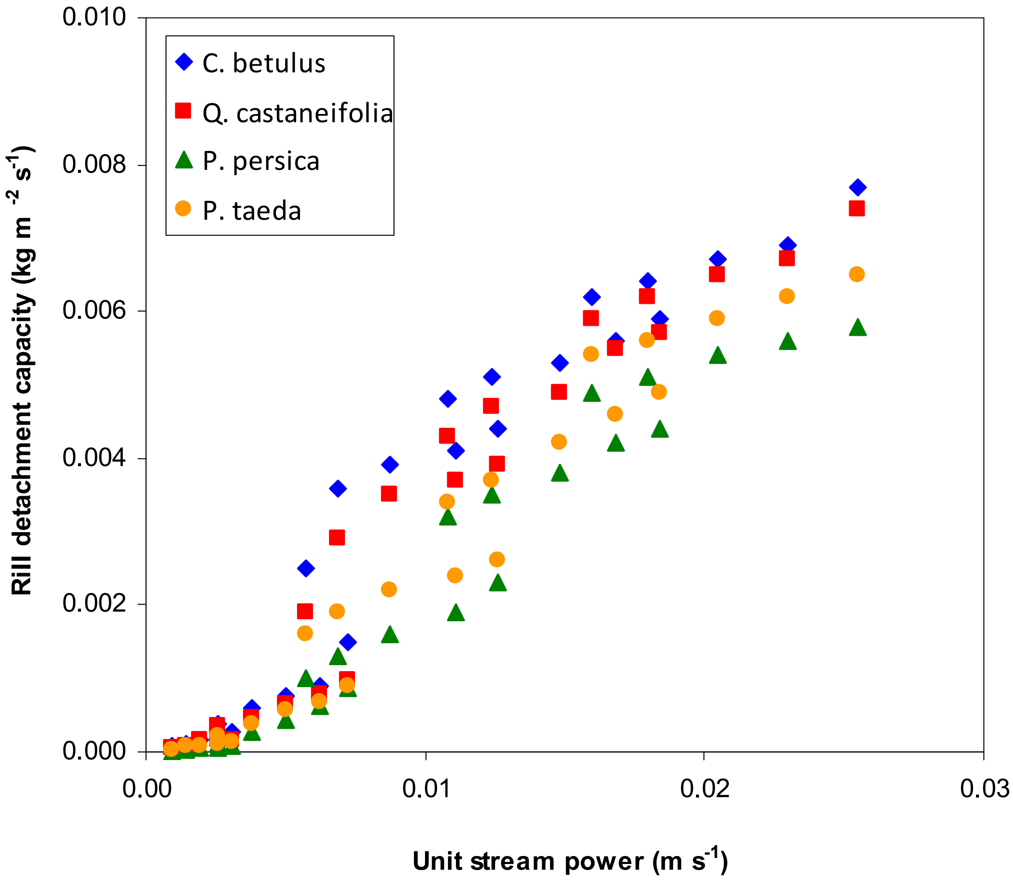

Figure 5 - Correlations between the rill detachment capacity and unit stream power in forest soils sampled under four tree species in Saravan Forest Park (Northern Iran) (n = 25 for each species).

In the previous study by Parhizkar et al. (2020a), the best predictor of D_c in forests was ω, and the interpolating equation was a power function. In this investigation, when the two variables were regressed using power equations, the coefficients of determination were high (R^2 > 0.85), but the prediction capacity of these equations (different for each tree species) was not always good, as shown by the values of E (> 0.75 only for *P. taeda*) (Tables 6 and 7). Adopting a linear equation, the values of R^2 and E increased for three of the four tree species. Only one model (for *P. persica*) was not accurate (E = 0.43), due to the large overestimation of D_c. The best model to predict D_c from ω was a logarithmic equation, for which all the evaluation indexes were good and the statistics (e.g., mean and maximum values) between predictions and observations were very close. However, in some cases (that is, at very low ω) the model gives negative values of D_c, and this suggests application only in the case of ω > 0.0025 m s^{-1}. This limitation is acceptable, because a low ω characterizes water flow with limited erosive power. In general, all the equations overestimated the observed D_c, as shown by the negative CRM, but the RMSE was always satisfactory (except for the linear equation applied to *P. persica*) (Tables 6 and 7).

Table 6 - The equations correlating D_c (kg m^{-2} s^{-1}) with the unit stream power (ω, m s^{-1}) in forest soils sampled under four tree species in Saravan Forest Park (Northern Iran) (*n* = 25 for each species).

Function	**Tree species**	**Equation**
Power	*C. betulus*	$D_c = 3.620\ \omega^{1.559}$
	Q. castaneifolia	$D_c = 4.673\ \omega^{1.640}$
	P. persica	$D_c = 17.744\ \omega^{2.024}$
	P. taeda	$D_c = 5.434\ \omega^{1.720}$
Linear	*C. betulus*	$D_c = 0.3487\ \omega + 0.0002$
	Q. castaneifolia	$D_c = 0.3420\ \omega + 0.0004$
	P. persica	$D_c = 0.3061\ \omega + 0.0006$
	P. taeda	$D_c = 0.2820\ \omega + 0.0006$
Logarithmic	*C. betulus*	$D_c = 0.0026 \ln \omega + 0.0163$
	Q. castaneifolia	$D_c = 0.0025 \ln \omega + 0.0156$
	P. persica	$D_c = 0.0020 \ln \omega + 0.1220$
	P. taeda	$D_c = 0.0022 \ln \omega + 0.0134$

Table 7 - Values of the criteria adopted for evaluating the accuracy of equations in Table 6 to predict the rill detachment capacity from the unit stream power in soils sampled under four tree species in Saravan Forest Park (Northern Iran).

Equation structure	**Tree species**	**Soil detachment capacity**	**Statistic**				**Index**			
			Mean	Minimum	Maximum	Standard deviation	R^2	E	CRM	RMSE
Power	*C. betulus*	*Observed*	0.0034	0.0001	0.0077	0.0026	0.85	0.71	-0.03	0.001
		Predicted	0.0035	0.0001	0.0119	0.0034				
	Q. castaneifolia	*Observed*	0.0031	0.0001	0.0074	0.0026	0.85	0.71	-0.03	0.001
		Predicted	0.0032	0.0000	0.0114	0.0032				
	P. persica	*Observed*	0.0023	0.0000	0.0058	0.0021	0.86	0.63	-0.11	0.001
		Predicted	0.0025	0.0000	0.0106	0.0029				
	P. taeda	*Observed*	0.0026	0.0000	0.0065	0.0023	0.90	0.82	-0.04	0.001
		Predicted	0.0027	0.0000	0.0099	0.0028				
Linear	*C. betulus*	*Observed*	0.0034	0.0001	0.0077	0.0026	0.92	0.90	-0.12	0.001
		Predicted	0.0038	0.0005	0.0091	0.0025				
	Q. castaneifolia	*Observed*	0.0031	0.0001	0.0074	0.0026	0.94	0.84	-0.26	0.001
		Predicted	0.0039	0.0007	0.0091	0.0025				
	P. persica	*Observed*	0.0023	0.0000	0.0058	0.0021	0.95	0.43	-0.65	0.002
		Predicted	0.0037	0.0009	0.0084	0.0022				

	P. taeda	*Observed*	0.0026	0.0000	0.0065	0.0023	0.96	0.78	-0.36	0.001
		Predicted	0.0035	0.0009	0.0078	0.0020				
Logarithmic	*C. betulus*	*Observed*	0.0034	0.0001	0.0077	0.0026	0.87	0.86	-0.05	0.001
		Predicted	0.0035	-0.0019	0.0068	0.0024				
	Q. castaneifolia	*Observed*	0.0031	0.0001	0.0074	0.0026	0.85	0.84	-0.07	0.001
		Predicted	0.0033	-0.0019	0.0064	0.0023				
	P. persica	*Observed*	0.0023	0.0000	0.0058	0.0021	0.80	0.80	-0.05	0.001
		Predicted	0.0024	-0.0018	0.0049	0.0019				
	P. taeda	*Observed*	0.0026	0.0000	0.0065	0.0023	0.90	0.82	-0.04	0.001
		Predicted	0.0027	0.0000	0.0099	0.0028				

506 Notes: R^2 = coefficient of determination; E = coefficient of efficiency of Nash and Sutcliffe; RMSE = Root Mean Square Error; CRM = Coefficient of Residual Mass.

When D_c was regressed on the shear stress τ using equation (6), the slope (the rill erodibility K_r) and intercepts (the critical shear stress τ_c) of soils were different among the tree species. These equations had coefficients of regression (R^2) between 0.48 and 0.52, always significant at $p < 0.05$ (Table 8 and Figure 5). The soils with *C. betulus* and *P. persica* showed the maximum (0.0025 s m^{-1}) and minimum (0.0019 s m^{-1}) values of K_r, respectively, corresponding to the minimum (0.28 Pa) and maximum (0.42 Pa) values of τ_c. K_r of the soil with *C. betulus* soil was 1.04, 1.19, and 1.31 times greater than *Q. castaneifolia*, *P. taeda*, and *P. persica* soils, while τ_c of soils under *P. persica* was 1.5, 1.3, and 1.1 times the values of *C. betulus*, *Q. castaneifolia*, and *P. taeda*, respectively (Table 8).

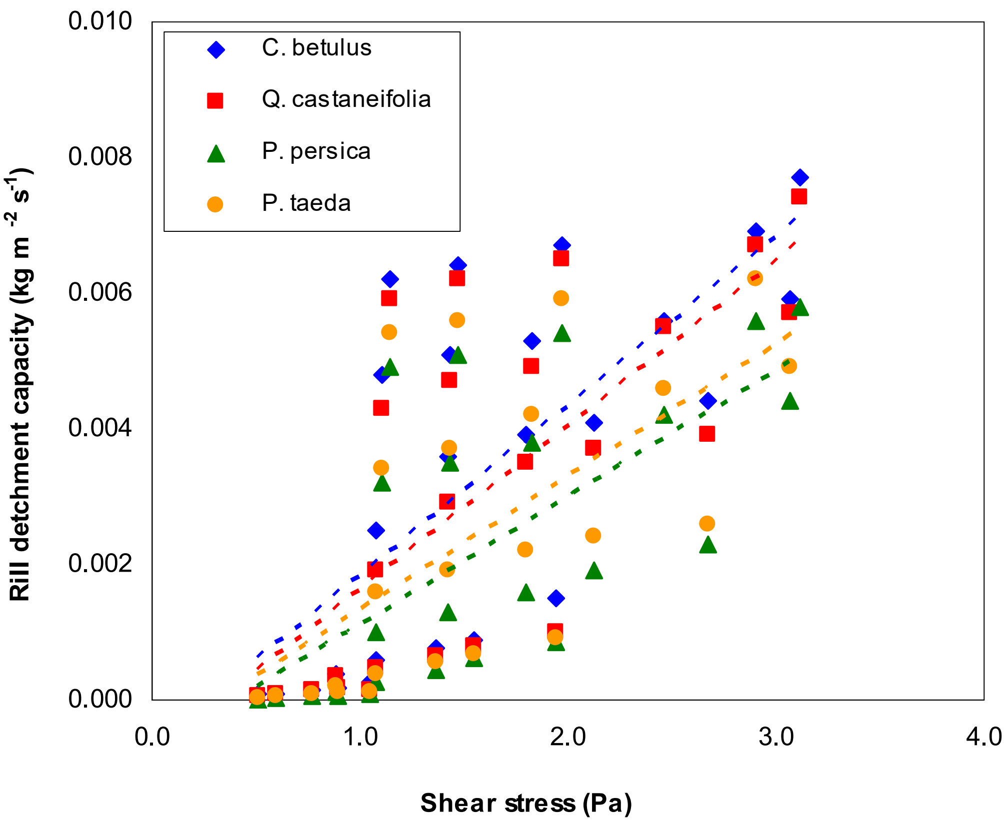

Figure 6 - Linear regression equations between the rill detachment capacity and the shear stress to estimate the rill erodibility and the critical shear stress in forest soils sampled under four tree species in Saravan Forest Park (Northern Iran) (*n* = 25 for each species).

Table 8 - Results of regression analysis between the rill detachment capacity (D_c) and the shear stress (τ) to estimate the rill erodibility (K_r) and the critical shear stress (τ_c) in forest

soils sampled under four tree species in Saravan Forest Park (Northern Iran) (n = 25 for each species).

Tree species	**Linear regression equation (6)**	K_r (s m^{-1})	τ_c (Pa)	R^2
C. betulus	$D_c = 0.0025\,\tau - 0.0007$	0.0025	0.28	0.52
Q. castaneifolia	$D_c = 0.0024\,\tau - 0.0008$	0.0024	0.33	0.52
P. persica	$D_c = 0.0019\,\tau + 0.0008$	0.0019	0.42	0.47
P. taeda	$D_c = 0.0021\,\tau - 0.0008$	0.0021	0.38	0.48

Note: R^2 = coefficient of determination.

4. Discussions

4.1. Effects of the tree species on soil properties and rill detachment capacity

The present study has explored whether four dominant tree species are able to induce changes in the erodibility of forest soils with homogenous texture (silty clay loam class) and similar properties (which are presumably due to the same forming processes and similar parent materials, Foth et al., 1990). Given this soil homogeneity, the plant survival and growth dynamics of the four tree species, combined with some practices used in this forest (such as forest improvement, timber harvesting, prescribed burning, and thinning), may explain the surveyed variations in the soil properties and rill detachment capacity.

The higher bulk density values and the lower aggregate stability of the soil with *C. betulus* could be due to the root system characteristics of this species. *C. betulus* has few surface roots (low weight density), which are responsible for a decrease in organic matter, strongly linked to the properties mentioned above. This is also confirmed by the correlation analysis, showing that, when the organic matter of soil increased, root system biomass and aggregate stability also increased. Conversely, soils with *P. persica*, which have a considerable surface roughness and structure (Viles et al., 1990; Gyssels et al., 2005), showed a higher root system biomass, organic matter content, and aggregate stability. Moreover, in these soils the bulk density was found to be lower, because the roots contribute to create a system of continuous pores (Gyssels et al., 2005, Angers and Caron, 1998; Shinohara et al., 2016). This result is in accordance with Shinohara et al. (2016) and David (2000), who showed that soil bulk density decreases with the presence of plant roots. Also Li et al. (1992; 1993) reported that fine roots less than one mm in diameter can significantly decrease the bulk density of soil and increase soil porosity). Furthermore, soil bulk density mainly depends on root diameter. As found by Meek et al. (1992), an increase in fine roots (less than one mm) implies a decrease in bulk density, while larger roots work in the opposite direction, which is consistent with several studies (e.g., Gyssels et al., 2005; Mamo and Bubenzer, 2001a; 2001b). In general, it has been demonstrated that species with high root density have the highest potential to reduce soil erosion rates by concentrated flow (De Baets et al., 2007).

The variability of the soil properties between the tree species having different root characteristics confirms that plant roots play a key role in driving changes in the soil. This leads to the conclusion that root density and structure, which vary among plant species, also exert an influence on soil detachment (Wang et al., 2015; Zhang et al., 2013; Li et al., 2015). In general, it has been demonstrated that rill erodibility and soil detachment rates decreased exponentially with root density (De Baets et al., 2007). More specifically, Wang et al. (2018b) found that soil detachment capacity decreases exponentially with root system biomass among two different types of root systems in grasslands. Li et al. (1991a) have demonstrated that soils with *Pinus tabulaeformis* (a conifer) and *Hippophae rhamnoides* (a typical tree and shrub in the Chinese Loess Plateau) show an exponentially decreasing trend of soil detachment by rills with root density. Also Gyssels and Poesen (2003) indicated that rill erosion decreases exponentially with increasing root densities of cereals and grasses in the loess Belt of Central Belgium, which is probably due to the combined effect of roots and shoots of vegetation on soil erosion. This influence results in noticeable changes in rill detachment capacity, which in this study varied significantly among the four tree species. The lowest root system biomass detected in soils with *C. betulus* explains the minor effect of this species on soil resistance to rill erosion. Additionally, exposing the soil with *C. betulus* to some management operations (e.g., prescribed burning, thinning) may have contributed to reducing the rill detachment capacity of this soil.

The lowest value of rill detachment capacity measured in soils with P. persica may be due to the highest root system biomass, and this is consistent with the results of other studies (Bibalani et al., 2006; Abdi et al., 2010). The latter authors found that the characteristics of the root system of *P. persica* enhance the stability of slopes by increasing the shear resistance of the soil, and this usually helps to minimize the risk of shallow landslides. Other studies (Wang et al., 2015; Li et al., 1991a; Li, 1995) have also concluded that plant roots are very important in reducing soil detachment, and specifically rill erosion (De Baets et al., 2005; Gyssels et al., 2005). The study by Wang et al. (2015) stated that plant roots have the greatest effect on increasing soil resistance to erosion, compared with other contributory factors. However, other investigations have shown that vegetation cover might not be so important or is even insignificant for controlling rill erosion (De Baets et al., 2007; Wang et al., 2014a). The fine and fibrous roots of *P. persica* increase soil stability and decrease its susceptibility to water erosion compared to the soils under other tree species. Moreover, root system biomass is commonly used to explain the influence of plant roots on soil detachment capacity. In this study, the highest root system biomass played more pronounced effects on the rill detachment capacity of soils with *P. persica* compared to the soils from the other tree species. The present study and the related literature indicate therefore that, for reducing rill erosion rates in erosion-sensitive areas (such as semi-arid forests) it is recommended to use plant species that develop a dense root network (i.e., with fibrous roots, De Baets et al., 2007). Moreover, management actions targeted at soil stabilization should be prioritized in these forest ecosystems, and deforestation, especially in *P. persica* areas, should be avoided to control soil erosion.

The correlation analysis and PCA confirmed the relationships between the most important properties and erodibility of the experimental soils. These statistical techniques demonstrated that, for the investigated tree species in forests, the rill detachment capacity was directly associated with the root system biomass and aggregate stability of sampled soils. This result is in accordance with Li et al. (1992a), who found that plant roots significantly increase soil's structural stability, and thus decreaseits erodibility. In other words, when root system biomass and aggregate stability decrease, rill detachment capacity increases.

Moreover, the three principal components provided by PCA individually synthesized the physical properties, the textural characteristics and the rill detachment capacity of soils. The clustering of soils in four groups (one for each tree species) showed a clear gradient according to the physical properties of the soil. Also in the studies of Lucas-Borja et al. (2020) and Shabanpour et al. (2020) - the latter carried out in the same environment - the differences in soil properties among different land uses (abandoned farmland, intensive cropland, grassland, forestland, and woodland) were evident, and well-differentiated groups, one for each land use, were clustered. In this study, these differences went beyond land uses (therefore the landscape scale) and down to a smaller spatial scale; this means that rill detachment capacity is different not only among different land uses (as several studies have demonstrated, e.g., Parhizkar et al., 202a; Shabanspour et al., 2020), but also among soils with a specific but dominant tree species, since the latter induces significant variations in soil's physical properties due to the action of its root system. This means that changes in soil properties, due to an individual tree species with its specific root actions, are important drivers of soil detachability in forests. A large body of literature shows that roots affect soil properties - such as infiltration rates, aggregate stability, water and organic matter contents, and shear strength - all controlling soil erosion rates to various degrees, not only in forests but in the majority of land uses (e.g., De Baets et al., 2007; Vogt et al., 1995; Lu et al., 2020).

In addition to the effects of tree root systems, soil erosion (and, therefore, the detachment component of this complex physical process) are influenced by other ecological characteristics of forest plants that drive soil hydrology. For instance, trees are also important in forest hydrology because of the interception of rainfall by their canopies, which reduces beneath-canopy throughfall and, ultimately, runoff and soil loss (Yang et al., 2019). In this regard, *P. persica*, *C. betulus* and *Q. castaneifolia*, although deciduous, have broad leaves that are arranged on the branches with a wide canopy, which increases interception (Nasiri et al., 2012). Conversely, the needles of *P. taeda* have a lower surface area that is not so effective at reducing canopy throughfall, but they do protect soil from the kinetic energy of intense storms, even in the wettest seasons. Moreover, the aboveground biomass of tree species can also reduce the hydrological response of soils, increasing hydraulic roughness and trapping sediments (Kervroëdan et al., 2018). All these characteristics of trees must be taken into account in addition to their root system features, when specific tree species have to be selected for erosion control.

4.2. Relationships between rill detachment capacity, rill erodibility, and unit stream power

Beside root characteristics and other hydrological factors linked to individual tree species, rill detachment capacity depends on the hydraulic characteristics of overland flow (Nearing et al., 1991). The regression analysis carried out in this study confirmed that unit stream power is a good predictor of rill detachment capacity. This high accuracy may be due to the fact that unit stream power simultaneously takes into account the flow velocity and soil slope, both influencing soil detachability due to overland flow (Parhizkar et al., 2020a). These results are in accordance with several studies, showing that rill detachment capacity by overland flow was closely related to flow characteristics, such as water discharge, shear stress, stream power, unit stream power, and unit energy; thus, rill detachment capacity can be estimated from one of these predictors (Nearing et al., 1991; Xiao et al., 2017; Li et al., 2019). Moreover, our results showed that, compared to the power equations identified in the previous study for forestls (Parhizkar et al., 2020a), a logarithmic function was more accurate at estimating the rill detachment capacity from the unit stream power for the different tree species. However, there is no physical reason for this higher accuracy, since our methodwas simply based on a "black-box" approach (Nearing et al., 1991), looking for the most accurate equation and the best predictor of a hydrological variable. This approach is used in several environmental studies, where the combination of complex physical, chemical and biological processes makes it practically impossible to create simulations on a mathematical basis, apart from simple regressions with variable analytical forms. The regression equations are site-specific, and must be calibrated and used in the same or a least in a very similar environment. The models are very useful for those users who require an order of magnitude of soil erodibility in a soil with a specific tree species.

The response curves of rill detachment capacity versus the hydraulic parameter chosen in this study (unit stream power) showed that the coefficients of the regression equations were very similar for three of the studied species (*C. betulus*, *Q. castaneifolia*, and *P. taeda*), while *P. persica* had a higher intercept (that is, rill detachment capacity in the case of zero stream power) and a lower slope (that is, rill detachment capacity increases less with unit stream power compared to the other species). This is further proof that soil erodibility is influenced not only by its physical properties, but also by the ecological features of plants, such as their root systems.

The rill detachment capacity of a soil due to overland flow is strictly linked to its rill erodibility and critical shear stress, which are two of the most important variables reflecting soil resistance to rill erosion (Nearing et al., 1989). In the context of the previous discussion, it is important to evaluate the effects of tree species in forests on these variables, which are highly sensitive input parameters of some process-based erosion models (Wang et al., 2016), such as the Water Erosion Prediction Project (WEPP) (Laflen et al., 1991). The regression equations set up in this study for the four tree species went in this direction, because they are the algorithm on which the erosion component of WEPP is based. Since rill erosion is the prevalent form in process-based erosion models, rill detachment capacity and erodibility are key parameters for accurate predictions of erosion (Wang et al., 2016; Nearing et al., 1989). Therefore, their quantification is important to improve the prediction accuracy of the WEPP model applications in arid areas.

However, the predictive accuracy of these equations, although satisfactory, was not as high as the models developed by Parhizkar et al. (2020a) and Zhang et al. (2008). Both these studies found that the linear regression functions between soil detachment and shear stress were very high for several land uses, with coefficients of determination of up to 0.9. Our study relates to a different spatial scale, and this may have influenced the lower prediction accuracy of the developed equations.

Compared to the other tree species, *P. persica* showed the lowest rill erodibility and the highest critical shear stress. This was an effect of the lowest rill detachment capacity, which was due to the binding effect of roots (Wang et al., 2014a), and of the changes induced by the root system on soil properties. In other words, the lower rill detachment capacity detected in *P. persica* soils, which was due to the interactive effects of roots and soil properties, also influenced the rill erodibility and critical shear stress, which were mathematically associated with the rill detachment capacity.

Among the root characteristics of all the tree specie, the density and diameter of *P. persica* provided the highest resistance of the soil to concentrated flow erosion. The lower rill erodibility in roots with a diameter lower than one mm, known as “effective” roots (Li et al., 1991b; 1992), was in accordance with previous studies, showing that these roots reduce concentrated flow erosion and thus decrease the soil detachment capacity (Li et al., 1991b; Li et al., 1995).

5. Conclusions

The soil’s physico-chemical properties (except soil texture and bulk density) and mean rill detachment capacity were different among the soils with four tree species sampled in Northern Iran. The soils with *Parrotia persica* and *Carpinus betulus* showed the lowest and the highest rill detachment capacity, respectively. This means the research question about the ability of the studied tree species with their root characteristics to reduce the rill detachment capacity compared to other plants can be confirmed. The higher root system biomass of *Parrotia persica* could have played a binding effect on the soil and improved its aggregate stability, thanks to the higher organic matter content. Therefore, *Parrotia persica* shows the highest capacity to protect soil against erosion. These results can support ecological engineers in the choice of tree species that are best indicated for soil conservation.

The most accurate equations to predict rill detachment capacity from unit stream power were based on a logarithmic function for all the studied species. These equations are highly accurate for water flow rates over 0.0025 m s^{-1}; this suitability addresses the second research question of this study. Rill erodibility and critical shear stress were lowest and highest, respectively, in *Parrotia persica*; this confirms the higher soil protection capacity against erosion of this species in comparison with the other plants. The proposed models are simple but quite accurate for predicting rill detachment rates. These models are particularly useful in ecological engineering applications, when the order of magnitude of soil erodibility must be estimated and the most effective plant species must be selected. However, further studies should be carried out to test the reliability of the suggested equations in other environmental conditions.

Acknowledgements

This study was funded by the Spanish Ministry of Economy, Industry and Competitiveness Research Projects, BIORESOC (CGL2017-88734-R). Isabel Miralles is grateful for funding received from the Ramón y Cajal Research Grant (RYC-2016-21191) from the Spanish Ministry of Economy, Industry and Competitiveness (MINECO).

References

Abdi, E., Majnounian, B., Genet, M., Rahimi, H., 2010. Quantifying the effects of root reinforcement of Persian Ironwood (Parrotia persica) on slope stability; a case study: Hillslope of Hyrcanian forests, northern Iran. Ecological Engineering. 36, 1409–1416.

Abdi, E., Deljouei, A., 2019. Seasonal and spatial variability of root reinforcement in three pioneer species of the Hyrcanian forest. Austrian Journal of Forest Science. 136 (3), 175-198.

Abdi, E., 2014. Effect of Oriental beech root reinforcement on slope stability (Hyrcanian Forest, Iran). Journal of forest science. 60 (4*)*, 166–173.

Abedi, R., Pourbabaei, H., 2011. Ecological species groups in the rural heritage museum of Guilan Province, Iran. Caspian J. Env. Sci. 9 (2*)*, 115–123.

Aksoy, H., Kavvas, M.L., 2005. A review of hillslope and watershed scale erosion and sediment transport models. Catena**.** 64, 247–271.

Amoopour, M., Ghobad-nejhad, M., Khodaparast, S.A., 2016. New records of polypores from Iran, with a checklist of polypores for Gilan Province. Czech Mycology. 68 (2), 139–148.

An, S., Mentler, A., Mayer, H., Blum, W.E., 2010. Soil aggregation, aggregate stability, organic carbon and nitrogen in different soil aggregate fractions under forestland and shrub vegetation on the Loess Plateau, China. Catena. 81, 226–233.

Angers, D.A., Caron, J., 1998. Plant-induced changes in soil structure: Processes and feedbacks. Developments in Biogeochemistry. 42, 55–72. doi:10.1023/A:1005944025343.

Asadi, H., Aligoli, M., Gorji, M., 2017. Dynamic changes of sediment concentration in rill erosion at field experiments. JWSS-Isfahan University of Technology. 20(78), 125-139.

Asadi, H., Ghadiri, H., Rose, C.W., Yu, B., Hussein, J., 2007. An Investigation of flow-driven soil erosion at low streampowers. J. Hydrol. 342, 134–142.

Asadi, H., Moussavi, A., Ghadiri, H., Rose, C.W., 2011. Flow-driven soil erosion processes and the size selectivity of sediment. J. Hydrol., 406, 73–81.

Bagnold, R.A., 1966. An approach to the sediment transport problem for general physics. In U.S. Geological Survey Professional Paper 422-I; U.S. Government Printing Office: Washington, DC, USA.

Berendse, F., Ruijven, J.V., Jongejans, E., Keesstra, S.D., 2015. Loss of Plant Species Diversity Reduces Soil Erosion Resistance. Ecosystems. 18(5), 881-888. DOI: 10.1007/s10021-015-9869-6.

Bibalani, G.H., Majnonian, B., Adeli, E., Sanii, H., 2006. Slope stabilization with Gleditshia caspica and Parrotia persica. Int. J. Environ. Sci. Tech. 2, 381-385.

Bonyad, A., 2006. Silvicultural Thinning Intensity Effects on Increasing the Growth of Planted Loblolly Pine (Pinus taeda L.) Stands in Northern Iran, Taiwan J For Sci, 21(3), 317-26.

Burylo, M., Hudek, C., Rey, F., 2012. Plant root traits affecting the resistance of soils to concentrated flow erosion. Earth Surface Processes and Landforms. 37, 1463-1470. Carter, M.R., 2002. Soil Quality for Sustainable Land Management: Organic Matter and Aggregation Interactions that Maintain Soil Functions. Agron. J. 94, 38–47.

Cerdà, A., González-Pelayo, O., Giménez-Morera, A., Jordán, A., Pereira, P., Novara, A., Brevik, E.C., Prosdocimi, M., Mahmoodabadi, M., Keesstra, S., García Orenes, F., Ritsema, C., 2016. The use of barley straw residues to avoid high erosion and runoff rates on persimmon plantations in Eastern Spain under low frequency – high magnitude simulated rainfall events. Soil Research 54, 154-165. DOI: 10.1071/SR15092.

David, D., 2000. Hydrologic effects of dryland shrubs: Defining the spatial extent of modified soil water uptake rates at an Australian desert site. Journal of Arid Environments. 45, 159-172.

De Baets, S., Poeson, J., Reubens, B., Wemans, K., de Baer-demaeker, J., Muys, B., 2008. Root tensile strength and root distribution of typical Mediterranean plant species and their contribution to soil shear strength. Plant and Soil. 307, 207–226.

De Baets, S., Poesen, J., 2010. Empirical models for predicting the erosion-reducing effects of plant roots during concentrated flow erosion. Geomorphology. 118, 425-432. DOI: 10.1016/j.geomorph.2010.02.011.

De Baets, S., Poesen, J., Gyssels, G., Knapen, A., 2006. Effects of grass roots on the erodibility of topsoils during concentrated flow. Geomorphology. 76, 54–67.

De Baets, S., Poesen, J., Knapen, A., Galindo, P., 2007a. Impact of root architecture on the erosion-reducing potential of roots during concentrated flow. Earth Surf. Process. Landf. J. Br. Geomorphol. Res. Group. 32, 1323–1345.

De Baets, S., Poesen, J., Knapen, A., Barberá, G. G., & Navarro, J. A. (2007b). Root characteristics of representative Mediterranean plant species and their erosion-reducing potential during concentrated runoff. Plant and Soil, 294(1-2), 169-183.De Leenheer, L. and De Boodt, M. 1959. Determination of aggregate stability by the change in mean weight diameter. Mededelingen van de Lundbouwhogeschool Gent, 24, 290-300.

Durán, Z.V.H., Francia, M.J.R., Rodríguez, P.C.R., Martínez, R.A., Cárceles, R.B., 2006. Soil erosion and runoff prevention by plant covers in a mountainous area (SE Spain): implications for sustainable agriculture. The Environmentalist. 26, 309–319.

Ellison, W.D., 1947. Soil erosion studies: Part I. Agric. Eng. 28, 145–146.

Fiener, P., Auerswald, K., 2003. Effectiveness of grassed waterways in reducing runoff and sediment delivery from agricultural watersheds. Journal of Environmental Quality. 32(3), 927-936.

Fortugno, D., Boix-Fayos, C., Bombino, G., Denisi, P., Quinonero Rubio, J. M., Tamburino, V., & Zema, D. A. (2017). Adjustments in channel morphology due to land-use changes and check dam installation in mountain torrents of Calabria (southern Italy). Earth Surface Processes and Landforms 42(14), 2469-2483.

Foster, G.R., 1982. Modeling the erosion process. In Hydrologic Modeling of Small Watersheds; Haan, C.T., Ed.; ASAE: St. Joseph, MI, USA, pp. 296–380.

Foth, H.D., 1990. Fundamentals of Soil Science, 8th ed. John Wiley and Sons: New York, NY, USA.

Geng, R., Zhang, G. H., Hong, D. L., Ma, Q. H., Jin, Q., & Shi, Y. Z. 2021. Response of soil detachment capacity to landscape positions in hilly and gully regions of the Loess Plateau. Catena, 196, 104852.

Gilman, E.F., Watson, D.G., 2014. Parrotia persica: Persian Parrotia. Environmental Horticulture Department, Florida Cooperative Extension Service, Institute of Food and Agricultural Sciences (IFAS), University of Florida, Gaineville FL 32611.

Google Earth V. 7.3.3.7786 (July 21, 2020). Saravan Forest Park, Iran. 37°08'10"N,49°40'18"E Eye alt. 916 m. DigitalGlobe 2020. https://earth.google.com [November 28, 2020] Govers, G., Everaert, W., Poesen, J., Rauws, G., De Ploey, J., Lautridou, J.P., 1990. A long flume study of the dynamic factors affecting the resistance of a loamy soil to concentrated flow erosion. Earth Surf. Process. Landf. 15, 313–328.

Grace III, J.M., 2002. Effectiveness of vegetation in erosion control from forest road sideslopes. Transactions of the ASAE. American Society of Agricultural Engineers. 45 (3), 681–685.

Gupta, H.V., Sorooshian, S., Yapo, P.O., 1999. Status of automatic calibration for hydrologic models: comparison with multilevel expert calibration. J. Hydrol. Eng. 4 (2), 135–143.

Gyssels, G., Poesen, J., 2003. The importance of plant root characteristics in controlling concentrated flow erosion rates. Earth Surf. Process. Landf. 28, 371–384.

Gyssels, G., Poesen, J., Bochet, E., Li, Y., 2005. Impact of plant roots on the resistance of soils to erosion by water: A review. Prog. Phys. Geogr. 29, 189–217.

Hacke, U.G., Sperry, J.S., Ewers, B.E., Ellsworth, D.S., Schäfer, K.V.R., Oren, R., 2000. Influence of Soil Porosity on Water Use in Pinus taeda. Oecologia 124(4), 495-505.

Herbrich, M., Gerke, H.H., Sommer, M., 2018. Root development of winter wheat in erosion-affected soils depending on the position in a hummocky ground moraine soil landscape. J. Plant Nutr. Soil Sci. 181, 147-157.

Hosseini, S.M., 2003. Incomparable roles of Caspian forests: heritage of humankind. Forest Sci., 3, 31-40.

IRIMO (Islamic Republic of Iran Meteorological Organization), 2016. Annual Rainfall Report. Available online: www.irimo.ir (accessed on 20 September 2019).

Jiao, J.Y., Tzanopoulos, J., Xofis, P., Mitchley, J., 2008. Factors affecting distribution of vegetation types on abandoned cropland in the hilly-gullied Loess Plateau region of China. Pedosphere. 18, 24-33.

Karimi, H.R., Sadeghi-Seresht, E., Nasrolahpour-Moghadam, S., Soleimani, S., Farahmand, H., Jome-Yazdian, M.S., 2018. Effects Chemical Treatments and Stratification on Seedlings Emergence of Persian Parrotia (Parrotia Persica (DC.) and Assessment of Genetic Diversity in its Seedlings, International Journal of Advanced Research in Botany, 4(3), 1-15.

Kartoolinejad, D., Hosseini, S.M., Mirnia, S.K., Akbarinia, M., Shayanmehr, F., 2007. The Relationship among Infection Intensity of Viscum album with some Ecological Parameters of Host Trees, Int. J. Environ. Res., 1(2), 143-149.

Keller, T., Håkansson, I., 2010. Estimation of reference bulk density from soil particle size distribution and soil organic matter content. Geoderma, 154, 398-406.

Kervroëdan, L., Armand, R., Saunier, M., Ouvry, J.F., Faucon, M.P., 2018. Plant functional trait effects on runoff to design herbaceous hedges for soil erosion control, Ecological Engineering, 118, 143-151.

Khanal, A., Fox, G.A., 2017. Detachment characteristics of root-permeated soils from laboratory jet erosion tests. Ecological Engineering. 100, 335-343.

Kooch, Y., Rostayee, F., Hosseini, S.M., 2016. Effects of tree species on topsoil properties and nitrogen cycling in natural forest and tree plantations of northern Iran, Catena, 144, 65-73.

Koskiaho, J., 2003. Flow velocity retardation and sediment retention in two constructed wetland–ponds. Ecological Engineering. 19(5), 325-337.

Kottek, M., Grieser, J., Beck, C., Rudolf, B., Rubel, F., 2006. World Map of the Köppen-Geiger climate classification updated. Meteorol. Z. 15, 259–263.

Krause, P., Boyle, D.P., Base, F., 2005. Comparison of different efficiency criteria for hydrological model assessment. Advances in Geosciences. 5, 89-97.

Laflen, J.M., Lane, J.L., Foster, G.R., 1991. WEPP–A New Generation of Erosion Prediction Technology. J. Soil Water Cons. 46 (1), 34-38.

Li, M., Hai, X., Hong, H., Shao, Y., Peng, D., Xu, W., Yang, Y., Zheng, Y., Xia, Z., 2019. Modelling soil detachment by overland flow for the soil in the Tibet Plateau of China. Sci. Rep. 9, 8063

Li, Y., Xu, X.-Q., Zhu, X.-M. and Tian, J-Y. 1992b. Effectiveness of plant roots on increasing the soil permeability on the Loess Plateau. Chinese Science Bulletin 37, 1735–38.

Li, Y., Xu, X.-Q. and Zhu, X.-M. 1993: Effective model on the roots of Chinese pine plantation to improve the physical properties of soil in the Loess Plateau. Scientia Silvae Sinicae 29, 193–98 (in Chinese).

Li, Y., 1995. Plant Roots and Soils Anti-Scourability on the Chinese Loess Plateau (in Chinese). Beijing, China: Science Press.

Li, Y., Tang, C., Wang, C., Tian, W., Pan, B., Hua, L., Lau, J., Yu, Z., Acharya, K., 2013. Assessing and modeling impacts of different inter-basin water transfer routes on Lake Taihu and the Yangtze River, China. Ecological engineering. 60, 399-413.

Li, Y., Zhu, X.M., Tian, J.Y., 1991a. Benefits of vegetation roots to improve erodibility in Loess Plateau (in Chinese). Science Bulletin. 36(12), 935-938.

Li, Y., Xu, X.Q., Zhu, X.M., 1992. Preliminary-study on mechanism of plant-roots to increase soil antiscouribility on the Loess Plateau. Sci. China Ser. B-chem. 35, 1085- 1092.

Li, Y., Zhu, X.M., Tian, J.Y., 1991b. Effectiveness of plant roots to increase the antiscourability of soil on the Loess Plateau. Chin. Sci. Bull. 24, 2077- 2082.

Li, Z.W., Zhang, G.H., Geng, R., Wang, H., Zhang, X.C., 2015. Land use impacts on soil detachment capacity by overland flow in the Loess Plateau, China. Catena. 124, 9–17.

Lu, J., Zhang, Q., Werner, A. D., Li, Y., Jiang, S., & Tan, Z. (2020). Root-induced changes of soil hydraulic properties–A review. Journal of Hydrology, 125203.

Lucas-Borja, M.E., Zema, D.A., Carrà, B.G., Cerdà, A., Plaza-Alvarez, P.A., Cózar, J.S., de las Heras, J., 2018. Short-term changes in infiltration between straw mulched and non-mulched soils after wildfire in Mediterranean forestland ecosystems. Ecol. Eng. 122, 27–31.

Mamo, M., Bubenzer, G., 2001a. Detachment rate, soil erodibility, and soil strength as influenced by living plant roots part I: laboratory study. Trans. ASAE. 44, 1167-1174.

Mamo, M., Bubenzer, G., 2001b. Detachment rate, soil erodibility, and soil strength as influenced by living plant roots part II: field study. Trans. ASAE. 44, 1175-1181.

Mao, Z., Saint-Andre, L., Genet, M., Mine, F.X., Jourdan, C., Rey, H., Courbaud, B., Stokes, A., 2012. Engineering ecological protection against landslides in diverse mountain forests: choosing cohesion models. Ecological Engineering. 45: 55–69.

Marvie-Mohadjer, M.R., 2019. Silviculture, 5th ed.; University of Tehran Press: Tehran, Iran, p. 418.

Meek, B.D., Rechel, E.R., Carter, L.M., DeTar, W.R., Urie, A.L., 1992. Infiltration rate of a sandy loam soil: Effects of traffic, tillage, and plant roots. Soil Science Society of America Journal. 56, 908-913.

Mirabolfathy, M., Javad, A., Ashnaei, P., 2018. The occurrence of Anthostoma decipiens, the causalagent of 'Carpinus betulus decline', in northern Iran, New Disease Reports, 37, 20. http://dx.doi.org/10.5197/j.2044-0588.2018.037.020.

Morgan, R., Quinton, J., Rickson, R., 1992. EUROSEM: Documentation Manual. Silsoe College, Silsoe, UK.

Moriasi, D.N., Arnold, J.G., Van Liew, M.W., Bingner, R.L., Harmel, R.D., Veith, T.L., 2007. Model evaluation guidelines for systematic quantification of accuracy in watershed simulations. Transactions of the ASABE. 50 (3), 885-900.

Moriasi, D.N., Arnold, J.G., Van Liew, M.W., Bingner, R.L., Harmel, R.D., Veith, T.L., 2007. Model evaluation guidelines for systematic quantification of accuracy in watershed simulations. Trans. ASABE. 50, 885–900.

Nash, J.E., Sutcliffe, J.V., 1970. River flow forecasting through conceptual models part I-a discussion of principles. J. Hydrol. 10, 282–290.

Nasiri, M., Zare, N., Jalilvand, H., 2012. Investigation of the effective factors on rate of stemflow for tree species in Hyrcanian forests, Egyptian Journal of Biology, 14, 37-44.

Nearing, M.A.; Foster, G.R.; Lane, L.J.; Finkner, S.C. A process-based soil erosion model for USDA-Water Erosion Prediction Project technology. Trans. ASAE 1989, 32, 1587–1593.

Nearing, M.A., Bradford, J.M., Parker, S.C., 1991. Soil detachment by shallow flow at low slopes. Soil Sci. Soc. Am. J. 55, 339–344.

Nearing, M.A., Foster, G.R., Lane, L.J., Finkner, S.C., 1989. A process-based soil erosion model for USDA-Water Erosion Prediction Project technology. Trans. ASAE. 32, 1587–1593.

Nearing, M.A., Norton, L.D., Bulgakov, D.A., Larionov, G.A., West, L.T., Dontsova, K.M., 1997. Hydraulics and erosion in eroding rills. Water Resour. Res. 33, 865–876.

Nearing, M.A., Simanton, J.R., Norton, L.D., Bulygin, S.J., Stone, J., 1999. Soil erosion by surface water flow on a stony, semiarid hillslope. Earth Surf. Process. Landf. 24, 677–686.

Norris, J. E., Di Iorio, A., Stokes, A., Nicoll, B. C., & Achim, A. (2008). Species selection for soil reinforcement and protection. In Slope stability and erosion control: ecotechnological solutions (pp. 167-210). Springer, Dordrecht.

Owoputi, L., & Stolte, W. (1995). Soil detachment in the physically based soil erosion process: a review. Trans. ASAE. 38 (4), 1099–1110.

Parhizkar, M., Shabanpour, M., Zema, D. A., & Lucas-Borja, M. E. (2020b). Rill Erosion and Soil Quality in Forest and Deforested Ecosystems with Different Morphological Characteristics. Resources, 9(11), 129.

Parhizkar, M., Shabanpour, M., Khaledian, M., Cerdà, A., Rose, C.W., Asadi, H., Lucas-Borja, M.E., Zema, D.A., 2020a. Assessing and Modeling Soil Detachment Capacity by Overland Flow in Forest and Woodland of Northern Iran. Forests. 11(1), 65.

Payam, H., Pourrajabali, S., 2020. Investigating the natural structures of Quercus castaneifolia C.A.Meyer in managed tracks in connection with physiographic factors in Northern Iran, Acta Ecologica Sinica, 40(2), 178-184.

Perez, J., Salazar, R. C., & Stokes, A. (2017). An open access database of plant species useful for controlling soil erosion and substrate mass movement. Ecological Engineering, 99, 530-534.

Picchio, R., Tavankar, F., Latterini, F., Jourgholami, M., Karamdost Marian, B., Venanzi, R., 2020. Influence of Different Thinning Treatments on Stand Resistance to Snow and Wind in Loblolly Pine (Pinus taeda L.) Coastal Plantations of Northern Iran, Forests, 11(10), 1034; https://doi.org/10.3390/f11101034.

Pollen, N., 2007. Temporal and spatial variability in root reinforcement of stream banks: accounting for soil shear strength and moisture. Catena. 69, 197–205.

Polyakov, V.O., Nearing, M.A., 2003. Sediment transport in rill flow under deposition and detachment conditions. Catena. 51, 33–43.

Prosdocimi, M., Cerdà, A., Tarolli, P., 2016. Soil water erosion on Mediterranean vineyards: a review. Catena. 141, 1–21.

Querejeta, J. I., Roldán, A., Albaladejo, J., & Castillo, V., 2001. Soil water availability improved by site preparation in a Pinus halepensis afforestation under semiarid climate. Forest Ecology and Management, 149(1-3), 115-128.

Raei, B., Asadi, H., Moussavi, A., Ghadiri, H., 2015. A study of initial motion of soil aggregates in comparison with sand particles of various sizes. Catena. 127, 279–286.

Rewald, B., & Rechenmacher, A., 2014. It's Complicated: Intraroot System Variability of Respiration and Morphological Traits in Four Deciduous Tree Species. Plant Physiol. 166, 736-745.

Sagheb-Talebi, K.h., Sajedi, T., Yazdian, F., 2005. Forests of Iran. Research Institute of Forests and Rangelands Publications, 2nd. Ed., 1-28.

Santhi, C., Arnold, J.G., Williams, J.R., Dugas, W.A., Srinivasan, R., Hauck, L.M., 2001. Validation of the SWAT model on a large river basin with point and nonpoint sources. J. Am. Water Resour. Assoc. 37 (5), 1169–1188.

Sefidi, K., Marvie Mohadjer, M.R., Etemad, V., Copenheaver, C.A., 2011. Stand characteristics and distribution of a relict population of Persian ironwood (Parrotia persica C.A. Meyer) in northern Iran, Flora - Morphology, Distribution, Functional Ecology of Plants., 206 (5), 418-422.

SDSD (Soil Science Division Staff), 2017. Soil Survey Manual; Ditzler, C., Scheffe, K., Monger, H.C., Eds.; USDA Handbook 18 Government Printing Office: Washington, DC, USA.

Shabanpour, M., Daneshyar, M., Parhizkar, M., Lucas-Borja, M.E., Zema, D.A., 2020. Influence of crops on soil properties in agricultural lands of northern Iran. Science of The Total Environment. 711, 134694.

Shi, Z.H., Fang, N.F., Wu, F.Z., Wang, L., Yue, B.J., Wu, G.L., 2012. Soil erosion processes and sediment sorting associated with transport mechanisms on steep slopes. J. Hydrol. 454, 123–130.

Shinohara, Y., Otani, S., Kubota, T., Otsuki, K., Nanko, K., 2016. Effects of plant roots on the soil erosion rate under simulated rainfall with high kinetic energy. Hydrological Sciences Journal. 61 (13), 2435–2442.

Singh, J., Knapp, H.V., Demissie, M., 2004. Hydrologic modeling of the Iroquois River watershed using HSPF and SWAT. ISWS CR 2004-08. Champaign, Ill. Illinois State Water Survey. http://www.sws.uiuc.edu/pubdoc/CR/ISWSCR2004-08.pdf (Accessed 14 February 2018).

Van Liew, M.W., Garbrecht, J., 2003. Hydrologic simulation of the Little Washita River experimental watershed using SWAT. Journal of the American Water Resources Association. 39, 413-426.

Van Liew, M.W., Garbrecht, J., 2003. Hydrologic simulation of the Little Washita River experimental watershed using SWAT. J. Am. Water Resour. Assoc. 39, 413–426.

Vannoppen, W., Vanmaercke, M., De Baets, S., Poesen, J., 2015. A review of the mechanical effects of plant roots on concentrated flow erosion rates. Earth Sci. Rev. 150, 666–678

Vannoppen, W., De Baets, S., Keeble, J., Dong, Y., & Poesen, J. (2017). How do root and soil characteristics affect the erosion-reducing potential of plant species?. Ecological Engineering, 109, 186-195.

Vieira, D.C.S., Serpa, D., Nunes, J.P.C., Prats, S.A., Neves, R., Keizer, J.J., 2018. Predicting the effectiveness of different mulching techniques in reducing post-fire runoff and erosion at plot scale with the RUSLE, MMF and PESERA models. Environmental Research. 165, 365-378.

Viles, H.A., 1990. The agency of organic beings: A selective review of recent work in biogeomorphology. In Vegetation and Erosion: Processes and Environments; Thornes, J.B., Ed.; Wiley: Chichester, UK, pp. 5–25.

Vogt, K. A., Vogt, D. J., Palmiotto, P. A., Boon, P., O'Hara, J., & Asbjornsen, H. (1995). Review of root dynamics in forest ecosystems grouped by climate, climatic forest type and species. Plant and soil 187(2), 159-219.

Wang, B., Zhang, G.H., Zhang, X.C., Li, Z.W., Su, Z.L., Yi, T., Shi, Y.Y., 2014a. Effects of near soil surface characteristics on soil detachment by overland flow in a natural succession grassland. Soil Sci. Soc. Am. J. 78, 589–597.

Wang, B., Zhang, G.H., Shi, Y.Y., Li, Z., 2015. Effects of Near Soil Surface Characteristics on the Soil Detachment Process in a Chronological Series of Vegetation Restoration. Soil Science Society of America Journal. 79(4), 1213-1222.

Wang, B., Zhang, G.H., Yang, Y.F., Li, P.P., Liu, J.X., 2018b. The effects of varied soil properties induced by natural grassland succession on the process of soil detachment. Catena. 166, 192–199.

Wang, B., Zhang, G.H., Shi, Y.Y., Zhang, X.C., 2014b. Soil detachment by overland flow under different vegetation restoration models in the Loess Plateau of China. Catena. 116, 51–59.

Wang, B., Zhang, G.H., Yang, Y.F., Li, F.F., Liu, J.X., 2018a. Response of soil detachment capacity to plant root and soil properties in typical grasslands on the Loess Plateau. Agric. Ecosyst. Environ. 266, 68–75.

Wang, D.D., Wang, Z.L., Shen, N., Chen, H., 2016. Modeling soil detachment capacity by rill flow using hydraulic parameters. J. Hydrol. 535, 473–479.

Wang, B., Li, P. P., Huang, C. H., Liu, G. B., & Yang, Y. F. Effects of root morphological traits on soil detachment for ten herbaceous species in the Loess Plateau. Science of the Total Environment, 754, 142304.

Wang, D.D.; Wang, Z.L.; Shen, N.; Chen, H. Modeling soil detachment capacity by rill flow using hydraulic parameters. J. Hydrol. 2016, 535, 473–479.

Xiao, H., Liu, G., Liu, P.L., Zheng, F.L., Zhang, J.Q., Hu, F.N., 2017. Response of soil detachment rate to the hydraulic parameters of concentrated flow on steep loessial slopes on the loess plateau of China. Hydrol. Process. 31, 2613–2621.

Yang, C.T., 1972. Unit stream power and sediment transport. J. Hydrol. Div. ASCE. 98, 1805–1826.

Yang, B., Lee, D.K., Heo, H.K., Biging, G., 2019. The effects of tree characteristics on rainfall interception in urban areas, Landscape and Ecological Engineering, 15, 289–296.

Zema, D.A., Bingner, R.L., Govers, G., Licciardello, F., Denisi, P., Zimbone, S.M., 2012. Evaluation of runoff, peak flow and sediment yield for events simulated by the AnnAGNPS model in a Belgian agricultural watershed. Land Degradation and Development 23(3), 205-215. https://doi.org/10.1002/ldr.1068.

Zhang, G.H., Tang, K.M., Ren, Z.P., Zhang, X.C., 2013. Impact of grass root mass density on soil detachment capacity by concentrated flow on steep slopes. Trans. ASABE 56, 927–934.

Zhang, G.H., Liu, B.Y., Liu, G.B., He, X.W., Nearing, M.A., 2003. Detachment of undisturbed soil by shallow flow. Soil Sci. Soc. Am. J. 67, 713–719.

Zhang, G.H., Liu, B.Y., Nearing, M.A., Huang, C.H., Zhang. K.L., 2002. Soil detachment by shallow flow. Trans. ASAE. 45, 351–357.

Zhang, G.H., Liu, G.B., Tang, K.M., Zhang, X.C., 2008. Flow detachment of soils under different land uses in the Loess Plateau of China. Trans. ASABE. 51, 883–890.

SUPPLEMENTARY DATA

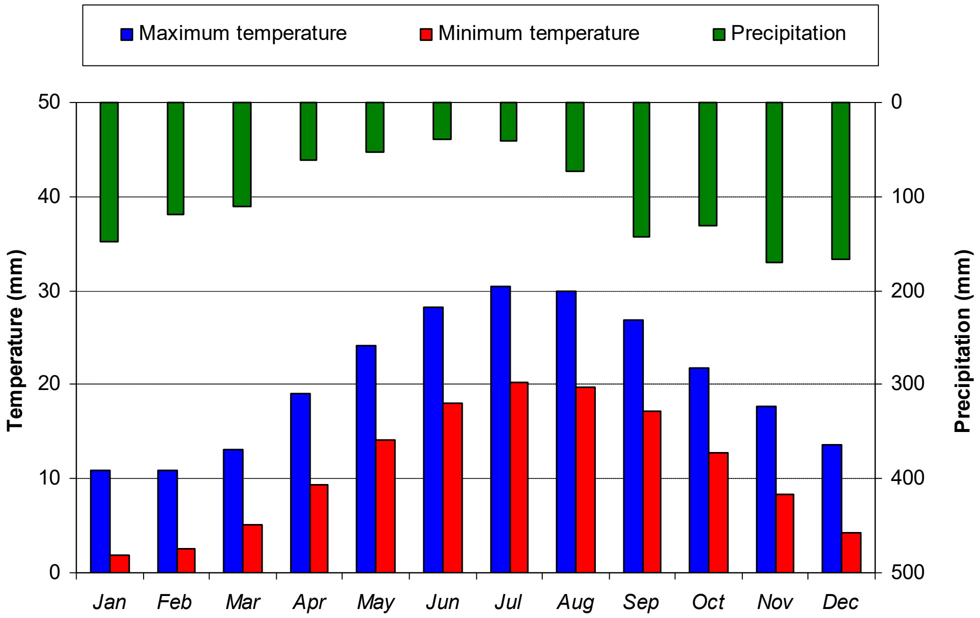

Figure 1(SD) – Mean values of monthly temperature and precipitation measured at the nearest meteorological station (records of the last 20 years) in Saravan Forest Park (Iran).

Table 1(SD) - Flow characteristics in the experiments carried out for measuring the rill detachment capacity under four tree species in Saravan Forest Park (Northern Iran).

Experiment	***S*** [m m^{-1}]	***q*** [L m^{-1} s^{-1}]	***h*** [m]	***R*** [m]	***V*** [m s^{-1}]	**τ** [Pa]	**Ω** [kg s^{-3}]	***ω*** [m s^{-1}]	**D_c** [kg s^{-1} m^{-2}]			
									C. betulus	***Q. castaneifolia***	***P. taeda***	***P. persica***
1		0.26	0.006	0.005	0.09	0.51	0.04	0.001	0.00001	0.00004	0.00006	0.00009
2		0.35	0.007	0.006	0.14	0.59	0.08	0.001	0.00003	0.00007	0.00009	0.00010
3	0.01	0.46	0.009	0.008	0.19	0.76	0.14	0.002	0.00005	0.00009	0.00015	0.00016
4		0.57	0.010	0.009	0.26	0.89	0.23	0.003	0.00006	0.00011	0.00017	0.00019
5		0.69	0.012	0.011	0.31	1.05	0.32	0.003	0.00008	0.00013	0.00015	0.00027
6		0.26	0.005	0.004	0.13	0.88	0.11	0.003	0.00011	0.00022	0.00034	0.00039
7		0.35	0.006	0.005	0.19	1.07	0.20	0.004	0.00027	0.00038	0.00047	0.00059
8	0.02	0.46	0.008	0.007	0.25	1.36	0.34	0.005	0.00044	0.00057	0.00066	0.00077
9		0.57	0.009	0.008	0.31	1.55	0.48	0.006	0.00062	0.00069	0.00078	0.00089
10		0.69	0.011	0.010	0.36	1.94	0.69	0.007	0.00086	0.00091	0.00099	0.00150
11	0.03	0.26	0.004	0.004	0.19	1.07	0.20	0.006	0.00100	0.00160	0.00190	0.00250
12		0.35	0.005	0.005	0.23	1.42	0.32	0.007	0.00130	0.00190	0.00290	0.00360
13		0.46	0.007	0.006	0.29	1.79	0.52	0.009	0.00160	0.00220	0.00350	0.00390
14		0.57	0.008	0.007	0.37	2.12	0.78	0.011	0.00190	0.00240	0.00370	0.00410

15		0.69	0.010	0.009	0.42	2.67	1.12	0.013	0.00230	0.00260	0.00390	0.00440
16		0.26	0.003	0.003	0.21	1.10	0.29	0.011	0.00320	0.00340	0.00430	0.00480
17		0.35	0.004	0.004	0.31	1.43	0.44	0.012	0.00350	0.00370	0.00470	0.00510
18	0.04	0.46	0.005	0.005	0.37	1.83	0.67	0.015	0.00380	0.00420	0.00490	0.00530
19		0.57	0.007	0.006	0.42	2.46	1.03	0.017	0.00420	0.00460	0.00550	0.00560
20		0.69	0.009	0.008	0.46	3.07	1.41	0.018	0.00440	0.00490	0.00570	0.00590
21		0.26	0.002	0.002	0.32	1.14	0.36	0.016	0.00490	0.00540	0.00590	0.00620
22		0.35	0.003	0.003	0.36	1.47	0.53	0.018	0.00510	0.00560	0.00620	0.00640
23	0.05	0.46	0.004	0.004	0.41	1.97	0.81	0.021	0.00540	0.00590	0.00650	0.00670
24		0.57	0.006	0.006	0.46	2.90	1.33	0.023	0.00560	0.00620	0.00670	0.00690
25		0.69	0.007	0.006	0.51	3.12	1.59	0.026	0.00580	0.00650	0.00740	0.00770

Notes: D_c = rill detachment capacity; h = flow depth; R = hydraulic radius; q = flow rate per unit width; S = slope gradient; V = average water flow velocity; τ = hydraulic shear stress; ω = unit stream power; Ω = stream power.